Vacuum 222 (2024) 113010

Contents lists available at ScienceDirect

Vacuum

journal homepage: www.elsevier.com/locate/vacuum

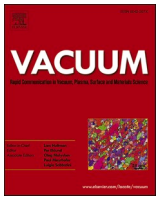

Surface modification of food-grade PVC monitored by angle-resolved XPS

G. Casula [a], M. Fantauzzi [a], B. Elsener [a], A. Rossi [a,*]

[a] Dipartimento di Scienze Chimiche e Geologiche, Università degli Studi di Cagliari, 09042, Cagliari, Italy

ARTICLE INFO

Handling Editor: Prof. L.G. Hultman

Keywords:
PVC
Polymer functionalization
Surface chemistry
Surface analysis
XPS
ARXPS

ABSTRACT

In this work the covalent functionalization of polyvinyl chloride (PVC) with (3-mercaptopropyl)trimethoxysilane (MPTMS) by nucleophilic substitution was investigated by X-ray photoelectron spectroscopy (XPS). The surface of food-grade PVC was characterized before and after treatment with ethanol and with 5% and 10% MPTMS solutions in ethanol. Special attention was paid to the determination of the chemistry, composition and thickness of the functionalized polymer surface by angle-resolved XPS (ARXPS). XPS analysis in standard mode and ARXPS spectra showed the presence of sulphur, silicon and oxygen from the MPTMS molecule. The quantitative analysis was in good agreement with the stoichiometry of the molecule. A small amount of chlorine, detected also at grazing angles, supported the formation of a layer, which resulted to be 2.2(0.2) nm thick including the hydrocarbon contamination usually detected by XPS on samples in contact with solutions. It is here demonstrated that XPS and ARXPS allow monitoring the surface functionalization and tune the conditions for achieving a good reproducibility during the functionalization of food-grade PVC by MPTMS. This is the starting point for further functionalization to obtain active food packaging with antimicrobial properties.

1. Introduction

X-ray photoelectron spectroscopy is acknowledged to be a powerful technique for the characterization of different materials including metals, alloys and polymers [1]. It is a surface sensitive method since it is possible to obtain information in the order of few nanometres ranging from 0.5 nm to 10 nm, depending on the material and on the emission angle. It provides the chemical state and the composition of the outermost layers of a material allowing monitoring the changes due to surface reactions as oxidation, compounds precipitation or formation of thin layer coatings with important improvements in the performance of the material. It can also be exploited for the characterization of multi-layered films by angle - resolved XPS mode [2]. One of the advantages of this technique is that it is almost non-destructive and it is well suited for investigating polymers that might be susceptible of degradation under x-ray irradiation [3]. A disadvantage is related to the fact that polymers are usually insulators and charge compensation is necessary to obtain the photoelectron spectra. Very often XPS is also used in combination with time-of-flight secondary ion mass spectroscopy (ToF-SIMS), which is more destructive than XPS but provides useful structural information complementary to those obtainable by XPS.

In food packaging industry there is an increasing interest in developing innovative materials that can preserve the quality and prolong the shelf-life of food and food products [4]. Food corruption and spoilage due to food-borne pathogens and microorganisms are reasons of concern for the food industry, consumers, and society as well. Food-grade polyvinyl chloride (PVC) is one of the most used polymers and in order to develop an active food packaging with antimicrobial properties, an active antimicrobial agent might be either introduced into a polymer

* Corresponding author.
E-mail address: rossi@unica.it (A. Rossi).

https://doi.org/10.1016/j.vacuum.2024.113010
Received 11 August 2023; Received in revised form 14 January 2024; Accepted 19 January 2024
Available online 9 February 2024

matrix or immobilised onto the polymer surface [5,6]. To this purpose a surface modification is usually required that enables the immobilization of an active agent. Several examples in literature show how antimicrobial agents can be covalently bonded on the polymer surface, such as guanidine-based cationic polymers [7], quaternary ammonium salts [8,9] or vanillin derivates [10]. Thanks to the presence of a C–Cl bond, a nucleophilic substitution reaction allows the immobilization of molecules containing specific functional groups, such as thiol groups, onto the polymer surface. The surface functionalization is affected not only by the composition of the substrate but also by many other parameters as the concentration of the functionalizing molecule, the solvent, the amount of water and the temperature.

The thickness of the functionalized layer on polymer surfaces is of interest in the investigation of antimicrobial and more in general antifouling layers. Parry and Shard proposed [11] a method based on ARXPS for the investigation of plasma treated surfaces. Also, the background shape analysis proposed by Tougaard [12] can be an interesting approach. Another method relies on the attenuation due to the overlayer (overlayer method = OM) [13].

The aim of this paper is to select the best analytical protocol based on X-ray photoelectron spectroscopy for determining and controlling the mechanism of surface functionalization of food-grade PVC with MPTMS. ARXPS was exploited for determining the thickness and the compositional depth profile in a non-destructive way. Furthermore, aspects related to sample degradation under ultra-high vacuum (UHV) conditions and under X-ray exposure are taken into account to provide evidence that the results are not affected by artefacts due to sample alteration. Indeed, it is known that chlorinated polymers may undergo sample degradation under X-ray in UHV due to loss of volatile compounds such as HCl [3,14]. Under the adopted conditions any ultra-high vacuum degradation was detected indicating that volatile compounds are not released by the polymer. Small variation on the Cl:CH–Cl atomic ratio was observed due to the exposure to the X-ray source.

2. Experimental

2.1. Materials

The chemical formulae of food-grade poly(vinyl)chloride (PVC) and of (3-mercaptopropyl) trimethoxy-silane (MPTMS) are shown in Figure 1:

Food-grade PVC samples were purchased from VWR (Italy) and cut in square pieces of 1 cm^2; no detailed information about type and quantity of plasticizers and stabilizers were available. (3-mercaptopropyl) trimethoxy-silane (MPTMS) and 96% ethanol were also from VWR (Italy). MPTMS is soluble in acetone and in ethanol while it is insoluble in water.

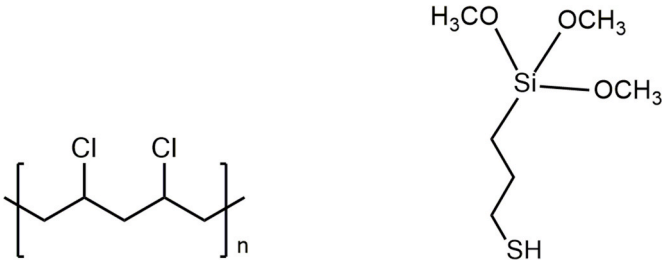

Fig. 1. Chemical formulae of poly(vinil) chloride (PVC) on the left and (3-mercaptopropyl) trimethoxy-silane (MPTMS) on the right.

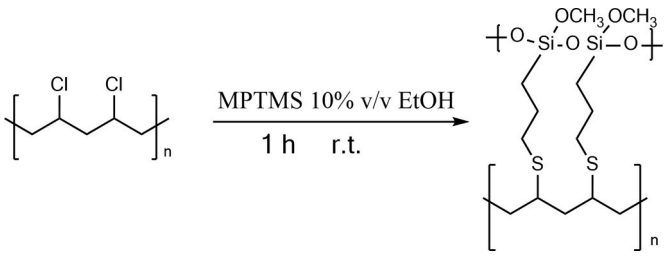

Fig. 2. Reaction scheme between PVC and MPTMS.

2.2. MPTMS functionalization

MPTMS modified PVC (M-PVC) samples were first obtained following the procedure reported by Villanueva et al. on medical grade PVC [14], which consists in the exposure of the PVC to a 5% v/v solution of MPTMS in acetone: water (75:25). That protocol has been modified in this work: ethanol was used to solubilize MPTMS instead of acetone: water (75:25), because acetone may lead to swelling and damage of the food-grade PVC.

Food-grade PVC samples were exposed to solutions of MPTMS 5% v/v and 10% v/v in ethanol for 1 h. The samples exposed to the solutions did not show physical changes visible to the naked eye. All the samples were washed in ethanol before the immersion in the MPTMS solutions and following 1 h of contact. The samples were left to dry at the open air, then they were mounted on a standard platen and transferred in the fast-entry air-lock of the spectrometer. These samples are named M-PVC 5% and M-PVC 10%, respectively. When PVC samples are exposed to a nucleophile such as thiol group, nucleophilic substitution reaction occurs, resulting in a surface modified PVC [15] according to the reaction scheme showed in Fig. 2.

2.3. X-ray photoelectron spectroscopy (XPS) and angle-resolved X-ray photoelectron spectroscopy (AR-XPS)

The XPS measurements were carried out with a Theta Probe spectrometer (Thermo Fisher Scientific, East Grinstead, UK). The spectra were collected under computer control [Avantage Software version 5.932 by Thermo Fischer] using a monochromatic $AlK_{\alpha 1,2}$ source ($h\nu$ = 1486.6 eV) selecting the nominal 400 μm spot size with a power of 100 W. Charge compensation was carried out using low energy electrons and argon ions. The base pressure into the XPS analysis chamber was $2x10^{-9}$ mbar but since the charge neutralization system requires Argon gas to be ionized, the residual pressure during the analysis was at $2x10^{-7}$ mbar. No changes in the residual pressure were observed during spectra acquisition.

All spectra were acquired in the fixed analyser transmission (FAT) mode, and pass energy (PE) was set at 200 eV for the survey spectra and at 150 eV for the high-resolution ones. Periodic calibrations were performed for verifying the linearity of the binding energy scale [ISO 15472:2010] and for determining the intensity/energy response function (IERF) that might drift upon time. The high-resolution spectra were resolved into their components using CASAXPS software V. 2.3.25 after background subtraction using U3-Tougaard iterative. Quantitative analysis to calculate the surface composition started with the experimental areas corrected for relative sensitivity factors that take into account the Scofield photoionization cross-section [16], the angular asymmetry factor of the photoemission from each atom [17], and the electron inelastic mean free path (IMFP, in nm) of the emitted electrons in the matrix M calculated according to Seah and Dench [18], using the following equation:

$$X_A = \frac{\frac{I_A}{S_A}}{\sum_{i=1}^{n} \frac{I_n}{S_n}} \quad (1)$$

Where X_A is the atomic fraction of the species A, I_A the intensity (area) of the photoelectron signal and S_A is the relative sensitivity factor.

Fresh-cut polyethylene terephthalate (PET) samples were used to test the charge compensation settings in both standard and angle resolved lens mode. This test was carried out before the spectra acquisition on the functionalized samples.

Since the use of adventitious carbon referencing has been pointed out as controversial in the literature [19], the binding energy scale was referred to the aliphatic C 1s peak assigned to the carbon of the long-chain of plasticizer/stabilizer present in the formulation of commercial food-grade PVC. This peak was taken at 285.0 eV as suggested in the literature [20] for aliphatic carbon. Degradation was always checked repeating the acquisition of the C 1s spectrum at the end of the XP-experiment, using the same instrumental settings used at the beginning for the first C 1s spectrum. Visual comparison between the first and the last C 1s scan was done for ascertaining that no degradation occurred.

To exclude PVC degradation due to the UHV conditions, the spectra of PVC samples immersed for 1 h in ethanol were analysed as soon as the samples were inserted into the analysis chamber and then after 72 h in UHV without being exposed to X-rays. Neither differences in the C 1s (Figure S1) and Cl 2p line-shapes nor in the Cl:CH–Cl (1:1) atomic ratio were observed.

High-resolution spectra in AR-XPS lens mode were acquired in parallel mode using 16 emission angles, ranging from 24.9°–81.1°. Emission angle is defined as the angle formed by the direction of the photoemitted electrons and the normal to the sample surface. Thickness calculation based on the ARXPS data was performed considering emission angles lower than 60° for limiting the elastic scattering influence [21–25] and for taking into account the surface roughness of the food-grade PVC. It is reported by Gunter et alii [24] that the influence of the sample roughness might be enhanced when measuring far from 45°.

3. Results

Survey spectra of as received PVC, ethanol washed PVC and of PVC following the various steps of the surface modification are shown in Fig. 3a.

3.1. Selection of the background model and XPS curve-fitting parameters

The selection of an appropriate background routine is crucial to ensure accurate and reliable results, representing a fundamental step in data processing as reported in Ref. [26]. In this work the background model was selected after comparing the Cl:CH–Cl atomic ratios obtained considering two background models: Shirley [23] and U 3 Tougaard [12,27,28].

When Shirley background was adopted, the Cl:CH–Cl atomic ratio resulted to be 0.8 and it was not in agreement with the expected 1:1 stoichiometry. Shirley algorithm assumes that the background intensity is proportional to the total intensity of the peak [29]. The three-parameters universal Tougaard-background (U 3 Tougaard in CASAXPS) relies on a quantitative description of the physical process that led to the background resulting more accurate for polymers and more in general for materials with narrow plasmons [12]. Using U 3 Tougaard background for processing the spectra of as received PVC and of PVC immersed in ethanol, FWHM height values did not change, while the Cl:CH–Cl atomic ratio is in good agreement with the expected stoichiometry as shown in Table 1 (columns 1 and 2). Among the line shapes available in CASA XPS, GL(30) has been chosen as also suggested in the literature for polymers [30].

The curve-fitting parameters and the constraints applied during the curve-fitting are reported in the supporting information (Table S1). The FWHM height of the C1s component ascribed to aliphatic C was allowed varying in the range 0.5–1.7 eV while the other components were linked so to have the same value of the first C1s signal. The FWHM height was usually found equal to 1.5 (0.1) eV as reported in Table S1. The FWHM height of O 1s components were linked and not constrained. As far as the Cl 2p signal, the Cl $2p_{3/2}$: Cl $2p_{1/2}$ area ratio was maintained equal to 2:1 and the FWHM height of each peak of the doublet was constrained to be the same.

In standard mode, the initial approach to resolving the C 1s high-resolution spectra primarily focused on considering only one aliphatic component related to the plasticizer at 285.0 eV. Lacking specific information about the formulation of PVC for food applications, it was assumed that the intensity of this component was 1.7 (0.1) times greater than that of C–Cl. Subsequently, all fits of the C1s in both standard mode and ARXPS were carried out by constraining the intensity of the C1s

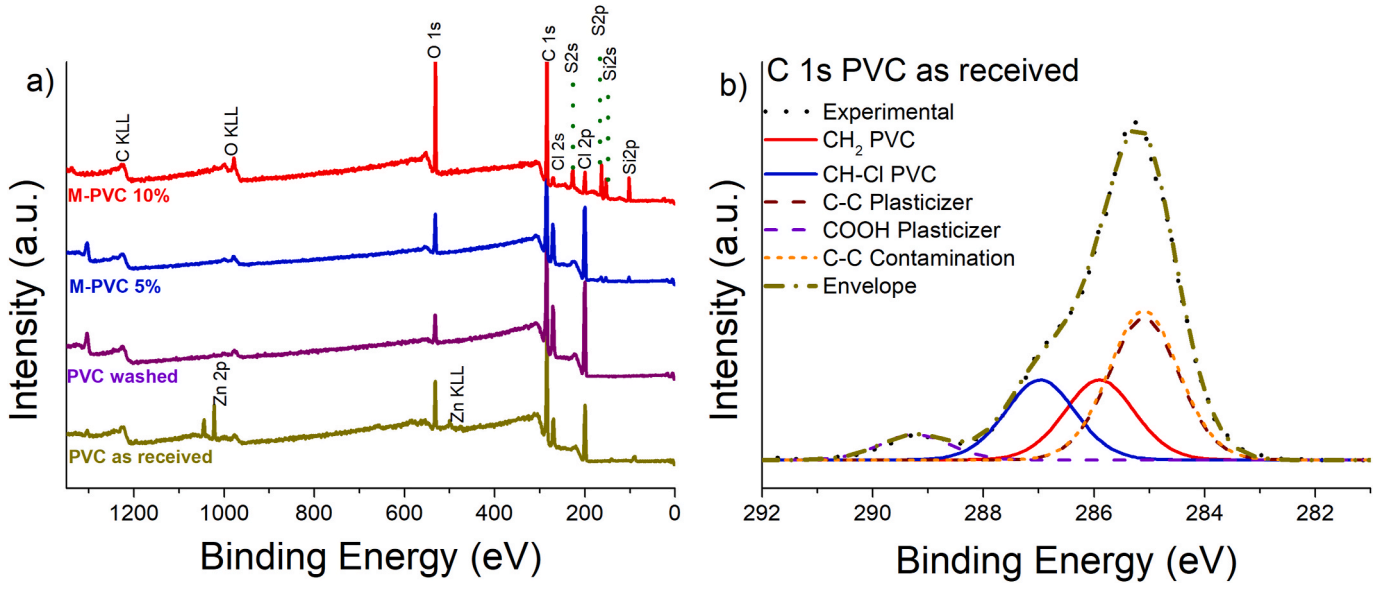

Fig. 3. (a): survey spectra of food-grade PVC "as received", after immersion in ethanol and functionalized with 5% and 10% MPTMS (b): example of a C 1s high-resolution spectrum of as received food-grade PVC.

Table 1
Quantitative results obtained from the spectra of as received PVC, food grade PVC after immersion in ethanol and M-PVC 10% The spectra were obtained in standard lens mode.

		as received PVC at%	washed PVC at %	M-PVC 10% at %	Theoretical at % calculated for PVC immersed in EtOH for 1 h
PVC (Bulk)	C contamination	25 (3)	25(4)	5 (3)	5
	C 1s CH_2 PVC	13 (2)	15 (1)	4 (1)	5
	C 1s CH–Cl PVC	13 (2)	15 (1)	4 (1)	5
	Cl 2p	13 (1)	17 (2)	5 (2)	5
	C 1s Carboxylate	4.1 (0.3)	4.1 (0.2)	2 (1)	1
	O 1s C=O	4.0 (0.2)	4 (1)	2 (1)	1
	O 1s C–O	4.0 (0.2)	4 (1)	2 (1)	1
	C 1s plasticizer	23 (3)	26 (1)	8 (2)	8
	Zn 2p	1 (0.2)	–	–	–
					Overlayer composition at%*
MPTMS (Overlayer)	C 1s C–Si, C–C	–	–	15 (1)	15
	C 1s C–S	–	–	15 (1)	15
	C 1s Methoxide	–	–	4 (1)	7
	O 1s Si–O–Si	–	–	16 (2)	18
	S 2p	–	–	7 (1)	7
	S 2p non grafted			1.0 (0.4)	–
	Si 2p	–	–	10 (1)	7

*Overlayer composition was calculated assuming 30% contribution of not functionalized substrate; this accounts for the layer architecture.

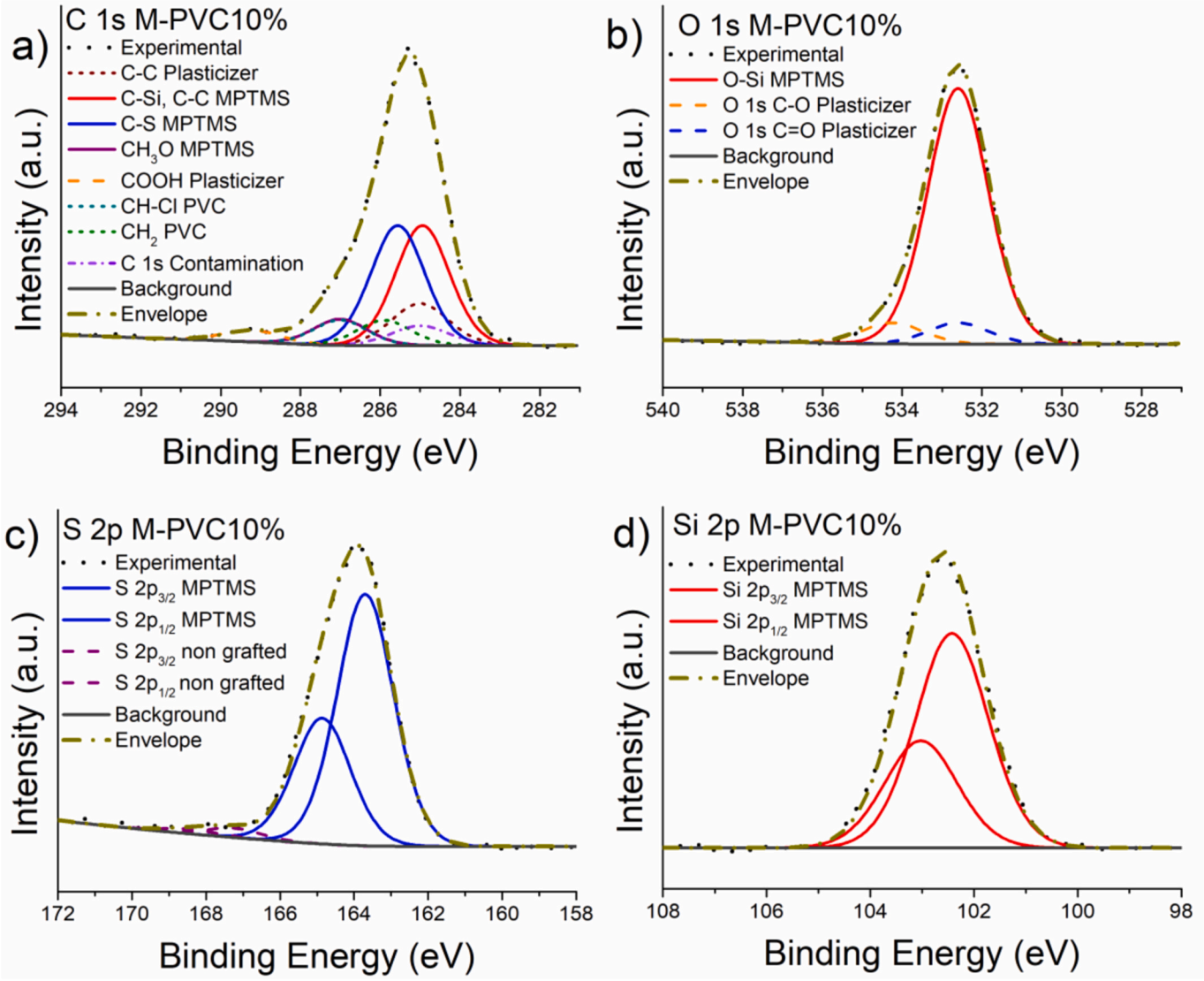

Fig. 4. High-resolution spectra of a) C 1s, b) O 1s, c) S 2p and d) Si 2p for M-PVC 10%.

from the plasticizer so to result 1.7 times more intense than that of the signal assigned to C–Cl. Any residual signals at that binding energy were attributed to contamination.

3.2. X-ray photoelectron spectroscopy of food-grade PVC before surface modification

In the as received samples, the signals of carbon (C 1s, C KLL) and chlorine (Cl 2p, Cl 2s) characteristic of PVC, are detected with those of the Zn 2p and Zn KLL and the O 1s ones due to the presence of zinc-based stabilizer/plasticizers. Following the immersion in ethanol, no zinc signals were revealed on the sample surface. The binding energy values of the elements are listed in Table S2.

An example of the high-resolution C 1s signal of "as received" food-grade PVC after background subtraction and curve-fitting is shown in Fig. 3b, the Cl 2p, O 1s and Zn 2p signals are provided in the supplementary materials (Fig. S2). Curve-fitting parameters for the Gaussian/Lorentzian curves were derived from spectra of reference compounds such as PET, analysed using the same experimental settings. The component at 287.0 eV has been assigned to the C–Cl [31] of the PVC and it has been fitted using one single peak with a full width at the half-maximum height (FWHM) of 1.55 eV. The component at 285.9 eV has the same intensity of the C–Cl component (1:1 ratio) and was assigned to the C–H carbon of the polymer. The component at 289.2 eV was attributed to the COOH group of the plasticizer [32]. The composition of the "as received" food grade PVC and of the PVC following the immersion in ethanol for 1 h are similar (see Table 1), the concentration of carbon in CH_2 groups, CH–Cl groups and chlorine are identical. It is worth to note that after immersion in ethanol for 1 h, the PVC did not show the zinc signal.

3.3. X-ray photoelectron spectroscopy of food-grade PVC after surface functionalization

XPS spectra were acquired following the immersion of the samples in the MPTMS solution for 1 h. Survey spectra of surface modified M-PVC 5% and M-PVC 10% (Fig. 3a) showed the presence of silicon (Si 2p, Si 2s) and sulphur (S 2p, S 2s) signals. The intensity of these signals from the MPTMS molecule is low in the case of sample M-PVC 5%. The signals of chlorine (Cl 2p, Cl 2s) from the PVC on the other side are still detected. Chlorine signals have a very low intensity in the sample following the immersion in the ethanol 10% MPTMS solution (named: M-PVC 10%) (Fig. 3a).

The high-resolution spectra of C 1s, O 1s, Si 2p and S 2p of the functionalized polymer M-PVC 10% were acquired for investigating the chemical state of the elements and for the quantification (Fig. 4). The binding energy values of the most intense photoelectron lines are provided in Table S2.

Following the functionalization with MPTMS the most intense components of the C1s signal (Fig. 4a), are C–C and C–Si (284.9 eV) and C–S (285.7 eV), both from the MPTMS molecule. The carbon signal at 285.0 eV, due to the plasticizer, is overlapped with the contribution of the surface contamination. Small signals from the underlying PVC were also detected (see Table 1).

O 1s signal (Fig. 4b) was fitted with three components: the component at 532.4 eV was assigned to oxygen bonded to the Si atoms [33] and two small components at about 532.3 eV and 534.2 eV were attributed to organic functional groups present in the formulation of the commercial food-grade PVC.

Fig. 4c and d shows the S 2p and Si 2p spectra for M-PVC 10%. The S 2p spectra (Fig. 4c) show two $2p_{3/2} - 2p_{1/2}$ doublets; for each doublet the energy separation was constrained to be 1.16 eV and the area ratio was constrained to be equal to 2:1. The binding energy of the most intense S $2p_{3/2}$ peak was found to be 163.7 eV and it is typical of thioether [34]. The second small component of the S $2p_{3/2}$ signal at 167.1 eV was attributed to non-grafted thiol group of MPTMS after an oxidative reaction of the sulphur [35]. The Si 2p peaks (Fig. 4d) were fitted with a doublet due to the spin-orbit coupling with an energy separation between the $2p_{3/2}$ and $2p_{1/2}$ components of 0.6 eV and an area ratio of 2:1.

The surface composition of the functionalized M-PVC 10% reflects both the functionalized MPTMS surface layer and the bulk PVC (Table 1).

The calculated at% of the MPTMS components, especially Si and S at %, suggested that not all chlorine of PVC have reacted. About 12% for silicon and sulphur would be expected for a complete reaction. The composition shown in Table 1 has been calculated assuming that 30% of the polymer surface did not react.

3.4. Angle-resolved X-ray photoelectron spectroscopy

Angle-resolved experiments were carried out on "as received" PVC, on M-PVC 5% and on M-PVC 10% to investigate the surface functionalization. On the as received PVC (Supplementary Material Figure S3), carbon, chlorine, oxygen, and zinc were detected at all emission angles. On the food-grade PVC samples immersed 1 h in ethanol the Zn signal was no more revealed (Supplementary Material Figure S4).

The presence of a contamination layer on the surface of PVC samples, which gives rise to the C 1s component located at 285 eV and labelled as "contamination" in Fig. 3b–is substantiated by ARXPS. The comparison of the spectra recorded at 24° and 58° (Figure S5) emission angles, shows that the intensity of that component increases with the emission angle, thus indicating that an adventitious contamination layer is present in the outermost part of the sample.

The ARXPS spectra of the functionalized M-PVC 10% are shown in Fig. 5. Apparent concentration in atomic percentage versus emission angle are reported in Fig. 6a for M-PVC 10%. It can be noted that the apparent concentration of Si 2p and the corresponding carbon atoms belonging to C–Si are nearly independent on the emission angle, indicating that these elements, that belong to the MPTMS molecule, are in the centre of the surface layer. The apparent concentration of sulphur S 2p, at the interface with the PVC, and even more that of chlorine Cl 2p, which belongs to the bulk PVC, decreases at high emission angle; on the contrary, the concentration of oxygen and of the CH_3O group increases. The relative depth plot (Fig. 6b), calculated by the Advantage software v. 5.932 (Thermo Fisher) based on the results of Fig. 6a, of the characteristic signals of MPTMS clearly shows that oxygen and silicon are at the outermost part of the layer, sulphur is in-between and chlorine is present at the greatest depth.

3.5. Determination of the thickness of the functionalized layer

Determination of the thickness of the functionalized layer is not straight-forward. Several possibilities based on XPS or ARXPS are proposed in literature [11,13,23]. Film thickness measurement of thin films on a substrate was proposed in 1970 by Hill et al. (Hill's equation) [36].

$$I_O = I_S\, e^{-\frac{t}{\lambda \cos\theta}} \tag{2}$$

In this equation t is the thickness of the overlayer, and θ is the photoelectron emission angle. The overlayer is assumed to be homogeneous in thickness and composition and the effective attenuation length λ of the photoelectrons is considered the same for the bulk and the overlayer, as is the case for systems where an oxide layer is present on the metallic substrate, e.g. SiO_2 on Si [37].

According to ISO 18115–1:2023, the effective attenuation length is defined as a "parameter which, when introduced in place of the inelastic mean free path into an expression derived for AES and XPS on the assumption that elastic scattering effects are negligible for a given quantitative application, corrects that expression for elastic scattering effects". The inelastic mean free path, IMFP, is defined by ISO 18115–1:2023 as the "average distance that an electron with a given energy travels between successive inelastic collisions". In our

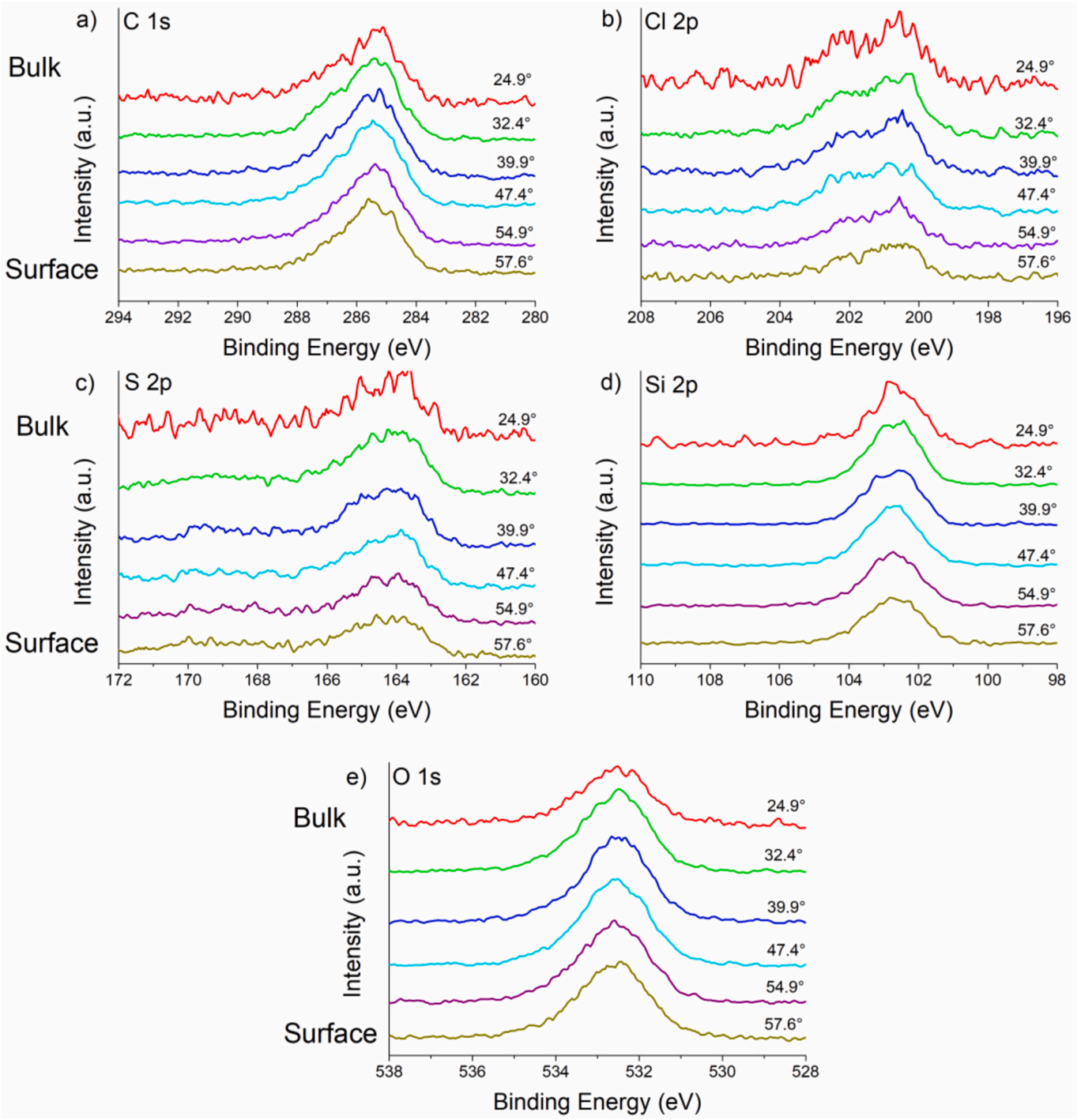

Fig. 5. Angle-resolved high-resolution C 1s, Cl 2p, S 2p, Si 2p and O 1s spectra of M-PVC 10% acquired at different emission angles.

calculations IMFP values are considered instead of the attenuation length since in the case of materials with low density, such as polymers, the effect of elastic scattering can be neglected. Furthermore, this approximation can be made because the thickness of the overlayer is supposed to be smaller than the IMFP [13].

As the system PVC substrate/MPTMS overlayer is more complex and no element (except the multi-component carbon) is present both in the bulk and in the overlayer, eq. (2) could not be applied in this work. The thickness was determined exploiting the attenuation of the chlorine Cl 2p signal, $I_{Cl,}$ (a single signal, no need of curve-fitting) measured at two emission angles, grazing (58°) and near perpendicular to the sample surface (24°). The formula is:

$$\ln\left(\frac{I_{Cl24^\circ}}{I_{Cl58^\circ}}\right) = -\frac{t}{\lambda_{Cl}}\left(\frac{1}{\cos\,(58^\circ)} - \frac{1}{\cos\,(24^\circ)}\right) \tag{3}$$

The thickness t of the overlayer thus results to be:

$$t = \frac{\ln\left(\frac{I_{Cl24^\circ}}{I_{Cl58^\circ}}\right) \bullet \lambda_{Cl}}{\cos(24^\circ) - \cos(58^\circ)} \tag{4}$$

The same formula was applied using, instead of chlorine Cl 2p, the intensities of sulphur S 2p (inner part of the functionalized layer) and of silicon Si 2p (outer part of the layer) to calculate the respective thickness. The IMFP, λ, for the different elements was calculated following

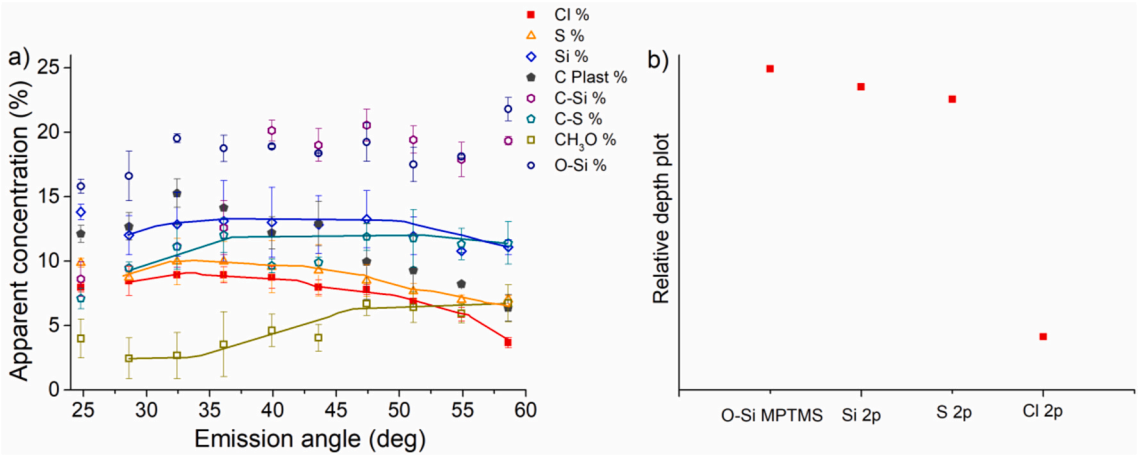

Fig. 6. Angle-resolved results acquired on M-PVC10%. Mean and standard deviation values were calculated using three independent measurements(a), relative depth plot (b).

Table 2
Layer thickness calculated based on the attenuation of the electrons emitted by Cl, S and Si using eq. (4), λ is calculated following Seah and Dench approach [18].

Element	Cl	S	Si
IMFP λ (nm)	3.12	3.16	3.24
Thickness (nm)	2.2 (0.4)	1.6 (0.4)	1.3 (0.4)

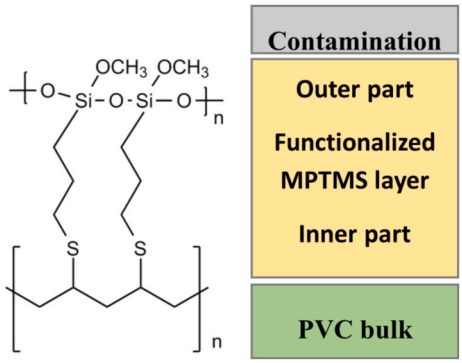

Fig. 7. Idealized model for the functionalized surface of food grade PVC with MPTMS.

Seah and Dench approach [18]. The thickness values, calculated on three independent samples having measured on each of them three points, are given in Table 2.

The total thickness based on the attenuation of chlorine is found to be 2.2 (0.4) nm; this value is the sum of the MPTMS layer, the contamination l_c and the underlying PVC substrate. The thickness of the MPTMS layer t plus contamination l_c is calculated based on the attenuation of the S 2p intensity and is found to be 1.6 (0.4) nm. Based on the attenuation of the Si 2p electrons the thickness of the outermost –OCH_3 groups plus the contamination layer l_c is 1.3 (0.4) nm (Fig. 7). The total thickness (calculated based on the intensities of chlorine) of the layer on top of the "as received" PVC was found to be 2.1 (0.8) nm and, for the PVC after immersion in ethanol, the total thickness of the layer was found to be 1.9 (0.7) nm.

4. Discussion

Based on the results presented above, a model for the functionalized food grade PVC samples can be proposed (Fig. 7). It consists in three layers: hydrocarbon layer due to the contamination on top, the functionalized layer containing the MPTMS molecule bonded via the sulphur atom to the PVC substrate, and the bulk PVC with plasticizer. Note that the interface between food-grade PVC and the functionalized layer might not be flat (as in the sketch Fig. 7) due to the fibrous structure of the polymer [38]. This might influence the calculated thickness values.

4.1. Influence of the synthesis protocol

It has been assessed in the literature [14] that PVC can be functionalized by exposing the sample to a nucleophilic group such as thiol groups; in that work the PVC samples were treated with a solution of MPTMS 5% in acetone: water (75:25) [14]. The exposure to acetone causes the degradation of the polymer, since acetone is a good swelling agent for PVC and leads to changes in the physical properties of the polymer [39]. As the food-grade PVC samples examined in this work had a lower thickness with respect to Ref. [14], acetone had to be avoided and as solvent was chosen ethanol. PVC shows a good resistance to ethanol at room temperature [40]. Indeed, binding energies (Table S2) and composition (Table 1) of the ethanol washed food-grade PVC do not change compared to the as received PVC and are in agreement with literature [3].

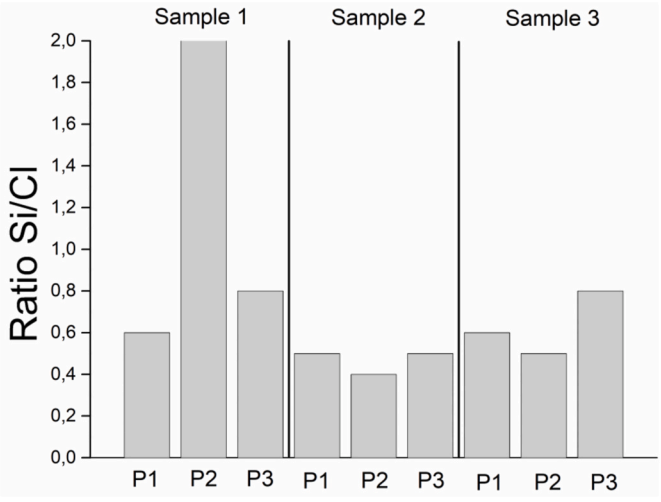

Fig. 8. Si 2p/Cl 2p atomic ratio of all measured points on M-PVC 10% (three samples - three analysis points each) indicating homogeneity of the functionalized layer (exception of point 2 of sample A).

4.2. Degree of functionalization – homogeneity of the MPTMS layer

Two different concentrations, 5% and 10%, of MPTMS in ethanol were used for the functionalization procedure. The XPS survey spectra (Fig. 3a) show that at 5% MPTMS the sulphur and silicon signals are less intense and the chlorine signals more intense than in case of samples treated in 10% MPTMS. This suggests that the functionalization reaction in 5% MPTMS might not be complete and the MPTMS only partially reacted with the PVC sample. The homogeneity of the surface was checked using the Si 2p to Cl 2p atomic ratio, where the signal of chlorine Cl 2p represents the bulk PVC and that of silicon Si 2p the MPTMS layer. For the M-PVC 5% samples, values of the Si 2p/Cl 2p ratio were in the range of 0.01–0.05 and a big scatter of the results obtained in the individual analysed areas (nominal diameter 400 μm) was found (Supplementary Material Figure S5), indicating low coverage and 50% of the areas with no or poor functionalization. For this reason, the procedure using 5% MPTMS solutions was considered not successful. The Si 2p to Cl 2p ratio for all analysed points on the three replicate samples of the sample M-PVC 10% as shown in Fig. 8 indicates that it is about 10 times higher and quite constant at 0.6 (0.1) than for the M − PVC 5%. This finding suggests the complete and homogeneous functionalization of the food grade PVC. Only one analysed point (P2 in sample 1) shows a high Si to Cl atomic ratio.

The chlorine concentration of functionalized samples M-PVC 10% was much lower than in "as received" food grade PVC, but chlorine could be still revealed (Fig. 3a–Table 1). The presence of the Cl 2p signal following the surface functionalization might be associated to chlorine atoms of the bulk PVC that were not involved in the nucleophilic reaction with sulphur (Fig. 1). Angle-resolved results shown in Fig. 5 confirm that chlorine is in the inner part of the M-PVC 10% samples, in fact, at high emission angles Cl atomic concentration decreases (Fig. 6a). The relative depth plot reported in Fig. 6b further confirms that Cl 2p signal is in the inner layers of the sample. The attenuation of the chlorine signal from the PVC due to an overlayer can be calculated considering different thicknesses of the surface layer d in standard conditions (emission angle is 53.6°). An apparent concentration of chlorine of 5 (1) %, that is in agreement with the chlorine concentration reported in Table 1, can be expected if an overlayer thickness of 2.2 nm is considered.

4.3. Thickness and composition of the functionalized layer

The total thickness of the functionalized surface layer on M-PVC 10% calculated with equation (4) is 2.2 (0.4) nm (Table 2). According to the proposed layered model (Fig. 7), the chlorine signal from the bulk PVC is attenuated by the bulk, by the MPTMS functionalized layer and by the contamination layer, thus the calculated total thickness of 2.2 (0.4) nm is the sum of the contamination layer l_c, of the MPTMS layer (here termed t) and includes the outer layer of PVC substrate. Applying equation (4) to the attenuation of sulphur (located at the interface between MPTMS layer and PVC) results in a thickness of 1.6 (0.4) nm that comprises the MPTMS layer t and the contamination layer l_c (Fig. 7). Applying the same equation to silicon (outer part of the MPTMS layer) a thickness of 1.3 (0.4) nm was obtained. This value corresponds to the contamination layer l_c plus few $–OCH_3$ groups located at the outer part of the MPTMS layer. Thus l_c can be estimated to be 1.1 nm, in agreement with the contamination layer thickness reported on PVC after sterilization (exposure to β-ray) [41].

Based on the difference between the thickness values of 1.6 nm (from sulphur atoms outwards) and the contamination l_c estimated to 1.1 nm, the measured thickness of the MPTMS layer t can be estimated to be equal to about 0.5 nm. The chain length of the MPTMS molecule (Fig. 2, Fig. 7) has been calculated with Avogadro software considering the distance between sulphur and oxygen of the monolayer and was found to be 0.8 nm; other work reported 0.9 nm estimated from bond length [42]. The lower thickness of the MPTMS layer measured by XPS in this work might indicate that the MPTMS molecules of the functionalized layer are not perpendicular to the substrate but they form an angle of about 25° with the normal to the PVC surface. Note that, according to eq. (3), the absolute values of t and l_c (Table 2) are relative to the IMFP λ – a higher value of λ would result (see eq. (4)) in higher absolute values. Furthermore, the difference in the t values calculated from ARXPS data and from Avogadro software, might be also influenced by the surface roughness of PVC samples (Figure S7). The effect of sample roughness for island type growth was discussed by Ref. [43]. Near to the so-called magic angle introduced by Gunter et al. who suggested a value of 45°, the surface roughness might cause minimal effects (estimated accuracy ±10%). The same functionalization reaction was conducted on fresh-cleaved polycrystalline gold having a roughness of 0.3 (0.1) nm measured by atomic force microscopy [44]. The estimated thickness of MPTMS on fresh-cleaved gold surface resulted to be 0.5 (0.1) nm in a very good agreement with the value obtained for the MPTMS on PVC (data to be published).

The composition of the functionalized food-grade PVC MPTMS surface layer (Table 1) comprises both the PVC and the functionalized MPTMS surface layer. Regarding the functionalized MPTMS surface layer, the composition is close to the stoichiometry; it can be noted that the concentration of the $O–CH_3$ groups (see Figs. 2 and 7) is much lower than the expected value based on the two-dimensional drawing of the MPTMS molecule (Fig. 1) where the silicon atoms are linked with only two bridging oxygen atoms. Taking into account three dimensional cross-linking as reported in Refs. [45–47], more Si–O bonds and less $O–CH_3$ groups would be present as is shown by the experiments (Table 1). The slight difference in the concentration (Table 1) between sulphur (7%) and silicon atoms (10%) might be explained by the stronger attenuation of sulphur located in the inner part of the MPTMS layer. Considering the ARXPS data and the relative depth plot (Fig. 6), the at% of oxygen slightly increases at higher emission angles, while silicon concentration remains nearly constant at all the emission angles and it is close to the concentration of 10% in standard mode (Table 1), substantiating its presence in the centre of the surface layer. Furthermore, sulphur concentration and more strongly chlorine concentration decrease at higher emission angles (Fig. 6), indicating that sulphur is located at the interface to PVC and chlorine is in the bulk of the polymer.

The exposure to the X-ray beam may lead to chlorine loss from the PVC during the experiment and this may affect the thickness calculation. Experiments were conducted on PVC samples after immersion in ethanol for 1 h to evaluate the loss of chlorine. The spectra are reported in Figure S6. The concentration (at%) of the component ascribed to the degradation, shown in Fig. S1, is about 2 at% after 50 min of exposure to X-ray. The degradation led to the decrease of the Cl:CH–Cl atomic ratio from 0.99 to 0.96 at the end of the experiment: such variation determines a small influence in the thickness estimation. The thickness of the MPTMS monolayer in this work was estimated to be 0.5 (0.1) nm and it is in agreement with the thickness determined with the same approach for a MPTMS monolayer on a freshly cleaved gold sample (roughness of 0.3 (0.1) nm [44]) as reported above.

5. Conclusions

In this work an analytical strategy based on XPS and ARXPS analysis for the in-depth characterization of the surface layer on food-grade PVC samples functionalized by MPTMS is proposed. The following conclusions can be drawn:

1. Detailed analysis of the XPS high-resolution spectra of M-PVC 10% suggests that functionalization of the polymer surface with MPTMS was successful and homogeneous. The composition of the MPTMS layer was close to the theoretical one but suggested a three-dimensional cross-linking of the Si–O–Si bonds.
2. Angle-resolved measurements confirmed the relative in-depth position of the functional groups of the monolayer. Based on these results a model of the functionalized surface was proposed. On the PVC bulk

a MPTMS monolayer of about 0.5 nm thickness is attached by nucleophilic substitution with the sulphur atoms, the MPTMS chains are oriented at an average value of about 25°. On top a hydrocarbon contamination layer of 1.1 nm is present.
3. Ethanol is an ideal solvent for carrying out surface functionalization of food-grade PVC, as the polymer is not damaged. A concentration of 10% v/v MPTMS in ethanol has been found to allow the achievement of a homogeneous functionalization of the polymer.

CRediT authorship contribution statement

G. Casula: Writing – original draft, Validation, Investigation, Formal analysis, Data curation. **M. Fantauzzi:** Writing – review & editing, Methodology, Conceptualization. **B. Elsener:** Writing – review & editing, Methodology, Conceptualization. **A. Rossi:** Writing – review & editing, Supervision, Project administration, Methodology, Funding acquisition, Conceptualization.

Declaration of competing interest

The authors declare that they have no known competing financial interests or personal relationships that could have appeared to influence the work reported in this paper.

Data availability

Data will be made available on request.

Acknowledgements

The authors are grateful to:
MIUR- Fondo per lo Sviluppo e la Coesione FSC-Piano Stralcio 2015/2017 for the Ph.D. grant assigned to Mr. Giulio Casula (Consortium UniCA and UniSS) – Project number CUP J89J20000930001 (2021): "Functionalization of Food Packaging with active antimicrobial agent" and to the University of Cagliari (UniCA) and Fondazione di Sardegna (FdS) for the financial support UNICA-FdS (Fondazione di Sardegna) 2019 – Project number CUP F72F20000240007.

Appendix A. Supplementary data

Supplementary data to this article can be found online at https://doi.org/10.1016/j.vacuum.2024.113010.

References

[1] D.N.G. Krishna, J. Philip, Review on surface-characterization applications of X-ray photoelectron spectroscopy (XPS): recent developments and challenges, Appl. Surf. Sci. Adv. 12 (2022) 100332, https://doi.org/10.1016/j.apsadv.2022.100332.
[2] V.P. Afanas'ev, D.N. Selyakov, O.Y. Ridzel, M.A. Semenov-Shefov, A.N. Strukov, Investigation of monolayer and submonolayer films using X-ray photoelectron spectroscopy, J. Phys. Conf. Ser. 1713 (2020) 012002, https://doi.org/10.1088/1742-6596/1713/1/012002.
[3] M. Manfredini, D. Atzei, B. Elsener, A. Marchetti, A. Rossi, Degradation of plasticized PVC for biomedical disposable device under soft x-ray irradiation, Surf. Interface Anal. 35 (2003) 294–300, https://doi.org/10.1002/sia.1532.
[4] S.H. Kamarudin, M. Rayung, F. Abu, S. Ahmad, F. Fadil, A.A. Karim, M.N. Norizan, N. Sarifuddin, M.S.Z. Mat Desa, M.S. Mohd Basri, H. Samsudin, L.C. Abdullah, A review on antimicrobial packaging from biodegradable polymer composites, Polymers 14 (2022) 174, https://doi.org/10.3390/polym14010174.
[5] J. Luna, A. Vílchez, Chapter seven - polymer nanocomposites for food packaging, in: R. Busquets (Ed.), Emerg. Nanotechnologies Food Sci., Elsevier, Boston, 2017, pp. 119–147, https://doi.org/10.1016/B978-0-323-42980-1.00007-8.
[6] L.J. Bastarrachea, D.E. Wong, M.J. Roman, Z. Lin, J.M. Goddard, Active packaging coatings, Coatings 5 (2015) 771–791, https://doi.org/10.3390/coatings5040771.
[7] F. Siedenbiedel, J.C. Tiller, Antimicrobial polymers in solution and on surfaces: overview and functional principles, Polymers 4 (2012) 46–71, https://doi.org/10.3390/polym4010046.
[8] M.E. Villanueva, A. Salinas, J.A. González, S. Teves, G.J. Copello, Dual antibacterial effect of immobilized quaternary ammonium and aliphatic groups on PVC, New J. Chem. 39 (2015) 9200–9206, https://doi.org/10.1039/C5NJ01766A.
[9] T. Min, Z. Zhu, X. Sun, Z. Yuan, J. Zha, Y. Wen, Highly efficient antifogging and antibacterial food packaging film fabricated by novel quaternary ammonium chitosan composite, Food Chem. 308 (2020) 125682, https://doi.org/10.1016/j.foodchem.2019.125682.
[10] H. Salmi-Mani, G. Terreros, N. Barroca-Aubry, C. Aymes-Chodur, C. Regeard, P. Roger, Poly(ethylene terephthalate) films modified by UV-induced surface graft polymerization of vanillin derived monomer for antibacterial activity, Eur. Polym. J. 103 (2018) 51–58, https://doi.org/10.1016/j.eurpolymj.2018.03.038.
[11] K.L. Parry, A.G. Shard, R.D. Short, R.G. White, J.D. Whittle, A. Wright, ARXPS characterisation of plasma polymerised surface chemical gradients, Surf. Interface Anal. 38 (2006) 1497–1504, https://doi.org/10.1002/sia.2400.
[12] S. Tougaard, Practical guide to the use of backgrounds in quantitative XPS, J. Vac. Sci. Technol. A 39 (2021) 011201, https://doi.org/10.1116/6.0000661.
[13] J. Walton, M.R. Alexander, N. Fairley, P. Roach, A.G. Shard, Film thickness measurement and contamination layer correction for quantitative XPS, Surf. Interface Anal. 48 (2016) 164–172, https://doi.org/10.1002/sia.5934.
[14] M.E. Villanueva, J.A. González, E. Rodríguez-Castellón, S. Teves, G.J. Copello, Antimicrobial surface functionalization of PVC by a guanidine based antimicrobial polymer, Mater. Sci. Eng. C 67 (2016) 214–220, https://doi.org/10.1016/j.msec.2016.05.052.
[15] T. Kameda, M. Ono, G. Grause, T. Mizoguchi, T. Yoshioka, Antibacterial effect of thiocyanate substituted poly(vinyl chloride), J. Polym. Res. 18 (2011) 945–947, https://doi.org/10.1007/s10965-010-9492-3.
[16] K.M.R. Kallury, P.M. Macdonald, M. Thompson, Effect of surface water and base catalysis on the silanization of silica by (Aminopropyl)alkoxysilanes studied by X-ray photoelectron spectroscopy and 13C cross-polarization/magic angle spinning nuclear magnetic resonance, Langmuir 10 (1994) 492–499, https://doi.org/10.1021/la00014a025.
[17] J.H. Scofield, Hartree-Slater subshell photoionization cross-sections at 1254 and 1487 eV, J. Electron. Spectrosc. Relat. Phenom. 8 (1976) 129–137, https://doi.org/10.1016/0368-2048(76)80015-1.
[18] M.P. Seah, W.A. Dench, Quantitative electron spectroscopy of surfaces: a standard data base for electron inelastic mean free paths in solids, Surf. Interface Anal. 1 (1979) 2–11, https://doi.org/10.1002/sia.740010103.
[19] D.R. Baer, K. Artyushkova, H. Cohen, C.D. Easton, M. Engelhard, T.R. Gengenbach, G. Greczynski, P. Mack, D.J. Morgan, A. Roberts, XPS guide: charge neutralization and binding energy referencing for insulating samples, J. Vac. Sci. Technol. A 38 (2020), https://doi.org/10.1116/6.0000057.
[20] C.D. Easton, C. Kinnear, S.L. McArthur, T.R. Gengenbach, Practical guides for x-ray photoelectron spectroscopy: analysis of polymers, J. Vac. Sci. Technol. A 38 (2020) 023207, https://doi.org/10.1116/1.5140587.
[21] P.J. Cumpson, M.P. Seah, Elastic scattering corrections in AES and XPS. II. Estimating attenuation lengths and conditions required for their valid use in overlayer/substrate experiments, Surf. Interface Anal. 25 (1997) 430–446, https://doi.org/10.1002/(SICI)1096-9918(199706)25:6<430::AID-SIA254>3.0.CO;2-7.
[22] J. Matthew, Surface analysis by Auger and x-ray photoelectron spectroscopy. D. Briggs and J. T. Grant (eds). IMPublications, Chichester, UK and SurfaceSpectra, Manchester, UK, 2003. 900 pp., ISBN 1-901019-04-7, 900 pp, Surf. Interface Anal. 36 (2004) 1647–1647. https://doi.org/10.1002/sia.2005.
[23] P.L.J. Gunter, O.L.J. Gijzeman, J.W. Niemantsverdriet, Surface roughness effects in quantitative XPS: magic angle for determining overlayer thickness, Appl. Surf. Sci. 115 (1997) 342–346, https://doi.org/10.1016/S0169-4332(97)00007-X.
[24] C.J. Powell, A. Jablonski, S. Tanuma, D.R. Penn, Effects of elastic and inelastic electron scattering on quantitative surface analyses by AES and XPS, J. Electron. Spectrosc. Relat. Phenom. 68 (1994) 605–616, https://doi.org/10.1016/0368-2048(94)80023-5.
[25] M.P. Seah, I.S. Gilmore, Simplified equations for correction parameters for elastic scattering effects in AES and XPS for Q, β and attenuation lengths, Surf. Interface Anal. 31 (2001) 835–846, https://doi.org/10.1002/sia.1113.
[26] M.H. Engelhard, D.R. Baer, A. Herrera-Gomez, P.M.A. Sherwood, Introductory guide to backgrounds in XPS spectra and their impact on determining peak intensities, J. Vac. Sci. Technol. Vac. Surf. Films 38 (2020) 063203, https://doi.org/10.1116/6.0000359.
[27] T.R. Gengenbach, G.H. Major, M.R. Linford, C.D. Easton, Practical guides for x-ray photoelectron spectroscopy (XPS): interpreting the carbon 1s spectrum, J. Vac. Sci. Technol. A 39 (2021) 013204, https://doi.org/10.1116/6.0000682.
[28] S. Tougaard, Universality classes of inelastic electron scattering cross-sections, Surf. Interface Anal. 25 (1997) 137–154, https://doi.org/10.1002/(SICI)1096-9918(199703)25:3<137::AID-SIA230>3.0.CO;2-L.
[29] D.A. Shirley, High-resolution X-ray photoemission spectrum of the valence bands of gold, Phys. Rev. B 5 (1972) 4709–4714, https://doi.org/10.1103/PhysRevB.5.4709.
[30] D. Briggs, Surface Analysis of Polymers by XPS and Static SIMS, Cambridge University Press, Cambridge, 1998, https://doi.org/10.1017/CBO9780511525261.
[31] E.D. Giglio, N. Ditaranto, L. Sabbatini, 2 Polymer surface chemistry: characterization by XPS, in: 2 Polym. Surf. Chem. Charact. XPS, De Gruyter, 2022, pp. 45–88, https://doi.org/10.1515/9783110701098-002.
[32] H. Hantsche, in: G. Beamson, D. Briggs (Eds.), High Resolution XPS of Organic Polymers, the Scienta ESCA300 Database, Wiley, Chichester, 1992, https://doi.org/10.1002/adma.19930051035, 295 pp., hardcover, £ 65.00, ISBN 0-471-93592-1, Adv. Mater. 5 (1993) 778–778.
[33] Y.-S. Li, W. Lu, Y. Wang, T. Tran, Studies of (3-mercaptopropyl)trimethoxylsilane and bis(trimethoxysilyl)ethane sol–gel coating on copper and aluminum, Spectrochim. Acta. A. Mol. Biomol. Spectrosc. 73 (2009) 922–928, https://doi.org/10.1016/j.saa.2009.04.016.

[34] H.J. Jang, C.-S. Park, E.Y. Jung, G.T. Bae, B.J. Shin, H.-S. Tae, Synthesis and properties of thiophene and aniline copolymer using atmospheric pressure plasma jets copolymerization technique, Polymers 12 (2020) 2225, https://doi.org/10.3390/polym12102225.

[35] A. Penna, M. Careri, N.D. Spencer, A. Rossi, Effects of tailored surface chemistry on desorption electrospray ionization mass spectrometry: a surface-analytical study by XPS and AFM, J. Am. Soc. Mass Spectrom. 26 (2015) 1311–1319, https://doi.org/10.1007/s13361-015-1135-9.

[36] J.M. Hill, D.G. Royce, C.S. Fadley, L.F. Wagner, F.J. Grunthaner, Properties of oxidized silicon as determined by angular-dependent X-ray photoelectron spectroscopy, Chem. Phys. Lett. 44 (1976) 225–231, https://doi.org/10.1016/0009-2614(76)80496-4.

[37] C.R. Brundle, G. Conti, P. Mack, XPS and angle resolved XPS, in the semiconductor industry: characterization and metrology control of ultra-thin films, J. Electron. Spectrosc. Relat. Phenom. 178–179 (2010) 433–448, https://doi.org/10.1016/j.elspec.2010.03.008.

[38] L. Mattoso, R. Offeman, D. Wood, W.J. Orts, E. Medeiros, Effect of relative humidity on the morphology of electrospun polymer fibers, Can. J. Chem. 86 (2008) 590–599, https://doi.org/10.1139/v08-029.

[39] 32 - polyvinyl chlorides (PVC), in: W.A. Woishnis, S. Ebnesajjad (Eds.), Chem. Resist. Thermoplast., William Andrew Publishing, Oxford, 2012, pp. 3177–3300, https://doi.org/10.1016/B978-1-4557-7896-6.00032-7.

[40] SR-94-27.pdf, (n.d.). https://erdc-library.erdc.dren.mil/jspui/bitstream/11681/12329/1/SR-94-27.pdf (accessed December 9, 2022).

[41] D. Atzei, B. Elsener, M. Manfredini, A. Marchetti, M. Malagoli, F. Galavotti, A. Rossi, Radiation-induced migration of additives in PVC-based biomedical disposable devices Part 2. Surface analysis by XPS, Surf. Interface Anal. 35 (2003) 673–681, https://doi.org/10.1002/sia.1590.

[42] S. Chaudhary, A.R. Head, J. Schnadt, X-Ray photoelectron spectroscopy study of adsorption of (3-mercaptopropyl)trimethoxysilane and N-propyltriethoxysilane on A rutile TiO2(110) surface, Adv. Mater. Lett. 6 (2015) 279–283, https://doi.org/10.5185/amlett.2015.SMS1.

[43] A.I. Martín-Concepción, F. Yubero, J.P. Espinós, S. Tougaard, Surface roughness and island formation effects in ARXPS quantification, Surf. Interface Anal. 36 (2004) 788–792, https://doi.org/10.1002/sia.1765.

[44] C. Passiu, A. Rossi, M. Weinert, W. Tysoe, N.D. Spencer, Probing the outermost layer of thin gold films by XPS and density functional theory, Appl. Surf. Sci. 507 (2020) 145084, https://doi.org/10.1016/j.apsusc.2019.145084.

[45] W.R. Thompson, M. Cai, M. Ho, J.E. Pemberton, Hydrolysis and condensation of self-assembled monolayers of (3-mercaptopropyl)trimethoxysilane on Ag and Au surfaces, Langmuir 13 (1997) 2291–2302, https://doi.org/10.1021/la960795g.

[46] I. Piwoński, J. Grobelny, M. Cichomski, G. Celichowski, J. Rogowski, Investigation of 3-mercaptopropyltrimethoxysilane self-assembled monolayers on Au(111) surface, Appl. Surf. Sci. 242 (2005) 147–153, https://doi.org/10.1016/j.apsusc.2004.08.009.

[47] V.V. Naik, M. Crobu, N.V. Venkataraman, N.D. Spencer, Multiple transmission-reflection IR spectroscopy shows that surface hydroxyls play only a minor role in alkylsilane monolayer formation on silica, J. Phys. Chem. Lett. 4 (2013) 2745–2751, https://doi.org/10.1021/jz401440d.